Location of the gel-like boundary in patchy colloidal dispersions: Rigidity percolation, structure, and particle dynamics

Javier A. S. Gallegos[*] and Román Perdomo-Pérez[†]
División de Ciencias e Ingenierías, Campus León, Universidad de Guanajuato, 37150 León, Guanajuato, Mexico

Néstor Enrique Valadez-Pérez[‡]
Facultad de Ciencias en Física y Matemáticas, Universidad Autónoma de Chiapas, 29050 Tuxtla Gutiérrez, Chiapas, Mexico

Ramón Castañeda-Priego[§]
Departamento de Ingeniería Física, División de Ciencias e Ingenierías, Campus León, Universidad de Guanajuato, 37150 León, Guanajuato, Mexico

(Received 5 November 2020; revised 18 September 2021; accepted 19 November 2021; published 10 December 2021)

During the past decade, there has been a hot debate about the physical mechanisms that determine when a colloidal dispersion approaches the gel transition. However, there is still no consensus on a possible unique route that leads to the conditions for the formation of a gel-like state. Based on gel states identified in experiments, Valadez-Pérez *et al.* [Phys. Rev. E **88**, 060302(R) (2013)] proposed rigidity percolation as the precursor of colloidal gelation in adhesive hard-sphere dispersions with coordination number $\langle n_b \rangle$ equal to 2.4. Although this criterion was originally established to describe mechanical transitions in network-forming molecular materials with highly directional interactions, it worked well to explain gel formation in colloidal suspensions with isotropic short-range attractive forces. Recently, this idea has also been used to account for the dynamical arrest experimentally observed in attractive spherocylinders. Then, by assuming that rigidity percolation also drives gelation in spherical colloids interacting with short-ranged and highly directional potentials, we locate the thermodynamic states where gelation seems to occur in dispersions made up of patchy colloids. To check whether the criterion $\langle n_b \rangle = 2.4$ also holds in patchy colloidal systems, we apply the so-called bond-bending analysis to determine the fraction of floppy modes at some percolating clusters. This analysis confirms that the condition $\langle n_b \rangle = 2.4$ is a good approximation to determine those percolating clusters that are either mechanically stable or rigid. Furthermore, our results point out that not all combinations of patches and coverages lead to a gel-like state. Additionally, we systematically study the structure and the cluster size distribution along those thermodynamic states identified as gels. We show that for high coverage values, the structure is very similar for systems that have the same coverage regardless the number or the position of the patches on the particle surface. Finally, by using dynamic Monte Carlo computer simulations, we calculate both the mean-square displacement and the intermediate scattering function at and in the neighborhood of the gel-like states.

DOI: 10.1103/PhysRevE.104.064606

I. INTRODUCTION

Colloidal dispersions are found in daily commercial products, like food, medicines, and construction materials, and in nature, like biological systems, for example, blood, cells, bacteria, among others, which exhibit both equilibrium and nonequilibrium thermodynamic phases, see, e.g., Ref. [1] and references therein. Thus, the understanding of the static properties and the transport phenomena of colloidal dispersions is of great importance in both science and technology [2–4]. Furthermore, colloids serve as model many-body systems, i.e., the interaction potential between colloids can be finely tuned in such a way that allows us to modify completely the macroscopic properties of the whole dispersion [1]. In particular, this manipulation at molecular level enables us to direct or to guide the shape and size of the main building blocks that define the organization or structure of the colloidal dispersions at large length scales [5].

Colloidal gels and glasses are the most prominent examples of dynamically arrested states, i.e., nonequilibrium states of matter [6], that exhibit a heterogeneous structure [1,7]. Despite the intensive research on colloidal gels [7], there is still an important discussion about the mechanisms that drive a colloidal dispersion into a gel-like state [8–15]. Of course, it is hard to think in a general or unique definition of gel that includes all possible kinds of colloidal systems. For example, from a macroscopic point of view, a gel exhibits a well-known rheological behavior [16]. However, nowadays, there is no a consistent and well-defined set of microscopic properties that allows us to establish a single criterion or route to determine

[*]ja.sanchezgallegos@ugto.mx
[†]r.perdomoperez@ugto.mx
[‡]nestor.valadez@unach.mx
[§]ramoncp@ugto.mx

if a colloidal dispersion can be considered as a gel or not. In fact, some important properties of colloidal gels, such as their elastic behavior and multiscale dynamics, have been recently unraveled [17,18] and, obviously, should be taken into account to specify all the ingredients that define a gel-like state.

Depending on the strength of the bonding, gels are classified as chemical or physical gels [7]. Chemical gelation, also called irreversible gelation, is well described in terms of percolation theory; one example is the case of polymeric chains, which grow by chemical reactions establishing a branched structure that spreads throughout all the available space [19]. However, in physical gels, the strength of the attraction is of the order of the thermal energy, therefore, bonds are continuously broken and formed in relatively short periods of time. Different routes of physical gelation have been proposed, they include the interruption of the spinodal decomposition [10,13] and the formation of a percolationlike state [11–13,15]. However, as mentioned above, there are specific conditions required to characterize a state as a physical gel [8,11,13,20].

The connectivity percolation is seen as a necessary but not a determining condition for gelation [21]. As mentioned above, in that thermodynamic state particle bonds are continuously formed and broken by the competition between the attractive forces and the thermal agitation, thus not being a sufficient condition to observe one of the fingerprints of gelation: the solidlike response when the material is under the action of mechanical perturbations. Therefore, colloidal gelation has to be linked to the formation of a mechanically stable network. This idea was proposed by two of us following the pioneering contribution of He and Thorpe [22], where a network-forming molecular material undergoes a covalent glass transition at the so-called rigidity percolation threshold and this occurs when the average number of bonds per particle, or coordination number $\langle n_b \rangle$, is equal to 2.4. More specifically, Valadez-Pérez *et al.* proposed that gelation in adhesive hard-sphere (AHS) dispersions is also the result of rigidity percolation [11]. This proposal was corroborated with gel states identified in experiments of colloids interacting with isotropic and short-ranged attractive forces [20,23]. Basically, Eberle *et al.* [20,23] determined the gel boundary in model nanoparticle dispersions with thermoreversible adhesive interactions with the assistance of small-amplitude dynamic oscillatory shear rheology and fiber-optics quasielastic light scattering experiments; the gel transition was defined using the Winter-Chambon rheological criterion [16] extended to colloidal systems, which states that the gel transition occurs when the slopes of the storage, G', and loss, G'', moduli as a function of the shear frequency become $1/2$ and equal. At this point, the dispersion experiences a transition from a Newtonian-like fluid to a Hookean-like solid; this is an important feature that defines the nature of a gel and its relationship with the formation of mechanically stable structures that should be observed when the dispersion reaches the gelation threshold.

Interestingly, in the case of weakly charged colloids immersed in a polymeric bath, i.e., a model for competing interaction systems, it has been shown that the gel state is also preceded by continuous and directed percolation (special case of connectivity percolation), which can also be linked with the bond distribution and a resulting coordination number that, in fact, is very near to 2.4 [12]. A recent study on the dynamical arrest in adhesive hard rod dispersions [14], another model system that has an interaction dependent on the shape of the particle, presented experimental evidence that gelation is also originated by rigidity percolation and basically occurs when $\langle n_b \rangle = 2.4$. As well as in the case of adhesive hard-sphere and hard-rod dispersions, the gel-like states are found at intermediate densities and above the gas-liquid coexistence curve, which means that they can be considered as homogeneous gels [20,23]. With this experimental corroboration, it is valid to ask whether rigidity percolation can drive colloidal gelation in systems with short-range and highly directional attractive forces.

In this contribution, we are interested in identifying those gel-like states in patchy colloidal dispersions by assuming that the criterion $\langle n_b \rangle = 2.4$ also holds regardless the number of patches and coverage. Although this is a pure heuristic criterion, we here discuss in detail the rich physical scenario that emerges under this assumption. Strictly speaking, we have located states that can be potentially considered as homogeneous gels of patchy particles. Once these states are estimated, it will be much easier to study their dynamical and mechanical properties. However, as we discuss further below, the validity of this a priori heuristic criterion is corroborated by implementing the so-called bond-bending analysis [24], which allows us to determine whether the percolating clusters generated by the condition $\langle n_b \rangle = 2.4$ are rigid or not, and thus to establish rigidity percolation as the precursor of colloidal gelation in attractive colloidal dispersions.

The use of patchy colloids in this work is twofold. First, the degree of anisotropy in the interaction potential, as discussed in the following section, can be easily adjusted [25]. Second, dynamical arrest and, in particular, gelation in a patchy colloidal system has not been investigated in detail. Nevertheless, in recent years, the effect of the surface heterogeneity on both the percolation threshold and gel formation has been studied by means of computer simulations [26,27]. Furthermore, due to the directional dependence of the potential, it has been predicted that this type of system exhibits an interesting thermodynamic behavior not observed in those systems composed of particles with only isotropic interactions [28] and new phases have emerged, for example, the so-called empty liquids [29–32]. The lack of experimental results on the gel formation in patchy colloids is mainly due to the synthesis of such kind of particles. However, recent advances in this direction have led the development of strategies to synthesize patchy colloids [33–35]; the most common difficulties related to the synthesis are the scalability, tunability and large-scale production [36].

The study of systems with nonisotropic interactions has been particularly relevant in the field of associating fluids where particles are limited to form only single bonds through association sites, see, for example, Ref. [37]. This kind of interaction eases the associating fluids description through theoretical approaches, such as the Wertheim perturbation theory [38]. This theory can also describe the behavior of particles with multiple interaction sites. In this work, we consider a more general interaction potential that allows multiple bonds between particles. The motivation for this choice is that particles with several number of patches, and different

coverages, present a variety of states not observed in simpler colloidal systems [29]. Besides, the experimental realization of those systems has become possible in the last years [30,39], which make them interesting colloidal model systems.

We have performed extensive Monte Carlo computer simulations for patchy colloidal dispersions to identify thermodynamic states where the condition $\langle n_b \rangle = 2.4$ is achieved. As we explain in detail further below, this is done by computing the mean energy per particle, which is proportional to the coordination number; the mathematical form of the interaction potential between patchy colloids allows us to properly define when two particles form a physical bond. However, for the identification of potential candidates of gel-like states, the existence of a cluster that spans the whole available volume is also necessary. Thus, algorithms capable of identify clusters have been also implemented. We have explored and located the boundary of gelation above the expected gas-liquid coexistence, and carried out an analysis of the structure and the particle dynamics along the gel-like states. The latter have been identified with rigidity percolation (RP), as suggested in various experiments of attractive colloidal systems [11,14]. In this contribution, rigidity percolation is also identified with the bond-bending analysis using the pebble game algorithm [24], which allows one to compute the fraction of floppy modes in the resulting percolating cluster. We should point out that this kind of analysis provides a mean-field approach to deal with the location of either rigid or gel-like states, therefore, we here use the concepts "mean-field rigidity" and "gel-like state" indistinctly. The results show evidence that the states near the $\langle n_b \rangle = 2.4$ curve are close the rigidity percolation threshold, giving to our assumption a very strong support.

Our findings show that the rigidity percolation threshold does not depend considerably on the number of patches and that not all patch coverages produce gel-like states; this information has important technological implications, for example, it is desired that some drugs remain in a liquid state to be injected into the bloodstream. We also find that systems of particles with the same patch coverage but different number of patches present a quite similar structure but their cluster size distribution is, in general, different. In fact, it is quite interesting that a simple criterion given by the coordination number provides a rich physical scenario that can explain both connectivity and rigidity percolation thresholds. Thus, our main findings point toward the rigidity percolation might be considered as the precursor mechanism of gelation in colloids with short-range attractive (isotropic and anisotropic) interactions. Furthermore, the transport properties, i.e., mean-square displacement and intermediate scattering function, along the RP curve do not show a glassy dynamics scenario, consistent with the physical picture observed in homogeneous gels [18].

II. POTENTIAL MODEL, COMPUTER SIMULATION DETAILS, STATIC AND DYNAMICAL PROPERTIES, AND SINGLE-BOND ANALYSIS

A. Kern-Frenkel potential

We have studied a system of patchy particles interacting through the so-called Kern-Frenkel potential [28]. The phase diagram and the structure of this kind of particles have been investigated using theoretical and simulation approaches for different number of patches, coverages and attraction ranges; see, e.g., Ref. [36] and references therein. In this model, the interaction potential $u_{ij}(\vec{r})$ between particles i and j is given by the product of an isotropic potential and an angular modulation as follows [28]:

$$u_{ij}(r_{ij}; \widetilde{\Omega}_i, \widetilde{\Omega}_j) = u_{ij}(r_{ij}) \times f(\widetilde{\Omega}_i, \widetilde{\Omega}_j). \tag{1}$$

The functional form of this potential allows us to tune the directional interaction, $f(\widetilde{\Omega}_i, \widetilde{\Omega}_j)$, independently of the radial interaction, $u_{ij}(r_{ij})$; r_{ij} is the relative distance between particles i and j, and $\widetilde{\Omega}$ is the particle orientation. We consider as the isotropic part the usual square well (SW) potential, u_{ij}^{SW}, between spheres of diameter σ [40],

$$u_{ij}^{SW}(r) = \begin{cases} \infty & \text{for } r < \sigma \\ -\epsilon & \text{for } \sigma \leqslant r \leqslant \lambda\sigma \\ 0 & \text{for } r > \lambda\sigma \end{cases}, \tag{2}$$

where λ and ϵ are the range and depth of the attraction, respectively. The attraction depth is controlled by the reduced temperature defined as $T^* = k_B T/\epsilon$, with k_B and T being the Boltzmann's constant and the absolute temperature, respectively. The angular modulation between any patches α and β on the surface of particles i and j, respectively, has the following mathematical form:

$$f(\widetilde{\mathbf{\Omega}}_\mathbf{i}, \widetilde{\mathbf{\Omega}}_\mathbf{j}) = \begin{cases} 1 & \text{if } \begin{cases} \hat{e}_\alpha \cdot \hat{r}_{ij} \leqslant \cos\delta \text{ for some patch} \\ \alpha \text{ in } i \\ \text{and } \hat{e}_\beta \cdot \hat{r}_{ji} \leqslant \cos\delta \text{ for some patch} \\ \beta \text{ in } j \end{cases} \\ 0 & \text{otherwise,} \end{cases} \tag{3}$$

where $\hat{r}_{ij}$ is the unitary vector that connects these two particles, $\hat{e}_\alpha$ and $\hat{e}_\beta$ are the unitary vectors in the normal direction to the patches α and β, respectively, and δ is called the aperture angle. The latter is related to the coverage fraction χ by Ref. [28],

$$\chi = n \sin^2\left(\frac{\delta}{2}\right), \tag{4}$$

where n is the number of patches on a colloid. The schematic representation of the Kern-Frenkel potential is given in Fig. 1(a). For this interaction potential, the reduced second virial coefficient, i.e., normalized with the second virial coefficient of hard-spheres; $B_2^{(\mathrm{HS})} = \frac{2\pi}{3}\sigma^3$, has an analytic representation given by Ref. [28],

$$B_2^* = 1 - \chi^2(\lambda^3 - 1)(e^{1/T^*} - 1). \tag{5}$$

We focus on particles with short-range attractions, namely, $\lambda = 1.1$ and 1.2, and different number of patches, n =1, 2, 3, 4, and 18. We have considered the following arrangements: for $n = 2$, patches are on the poles; for $n = 3$, patches form an equilateral triangle on a maximum circle around the particle; for $n = 4$, patches form a regular tetrahedron and for $n = 18$, patches are symmetrically distributed over the particle surface, see Fig. 1(b). Particles with 18 patches resemble the isotropic interaction, while particles with only one patch describes the most directional interaction. We have particularly chosen a few coverage sizes, ranging from 0.2 to 0.8. This

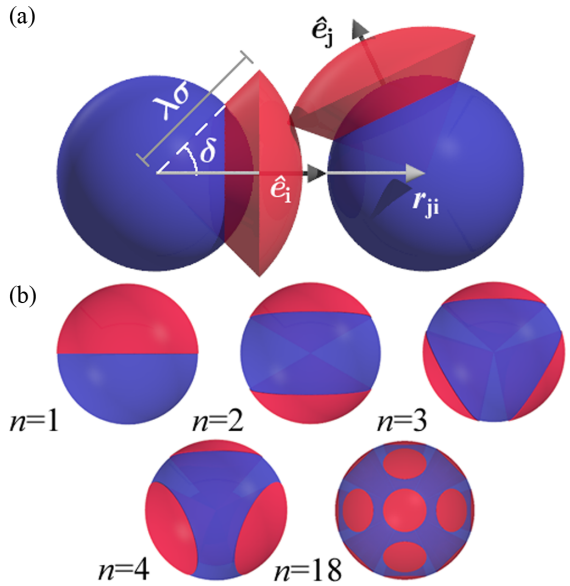

FIG. 1. (a) Schematic representation of patchy particles. Patches are modeled as spherical sections with radius $\lambda\sigma$ and aperture angle δ in the direction of the normal unitary vector $\hat{e}$. Two particles attract each other if the volumes of their patches overlap, otherwise the interaction is the usual hard core. (b) Representation of the five patchy geometries considered in this work. Here, patches cover 50% of the particle surface.

is related with the fact that the number of bonds per particle is relatively high, so small coverages never permit a large number of bonds because the geometric constriction and the short range nature of the potential, as we will discuss it below. For $n = 3$, the case $\chi = 0.8$ is discarded because the patches on the same particle slightly overlap due to their distribution on the particle surface. Therefore, for the sake of clarity, we have excluded the cases where patches overlap.

B. Monte Carlo computer simulations

We have carried out standard Monte Carlo (MC) computer simulations in the NVT ensemble with periodic boundary conditions. We simulated systems of particles with diameter σ inside a cubic simulation box. Systems consist of $N =$ 1000–2744 spheres. and the size L of the simulation box was set according to the reduced bulk density ρ^*, which is defined as $\rho^* = N\sigma^3/L^3$. The initial configuration for all simulations was a simple cubic crystalline arrangement with the appropriate constant spacing between particles.

A simulation run consists of N_{att} attempts of displacing particles and M_{att} attempts to rotate them. During the simulation, the probability of displacing or rotating a particle is the same. The initial displacement is chosen within the interval $-0.1\sigma \leqslant \Delta l \leqslant 0.1\sigma$ and the rotation angle takes the values -0.1 rad $\leqslant \Delta\theta \leqslant 0.1$ rad. Both Δl and $\Delta\theta$ are adjusted separately to have an acceptance ratio of 50%. A typical simulation run consists of 4×10^6 MC steps to reach the equilibrium and 6×10^6 MC steps to gather statistics and perform the ensemble averages.

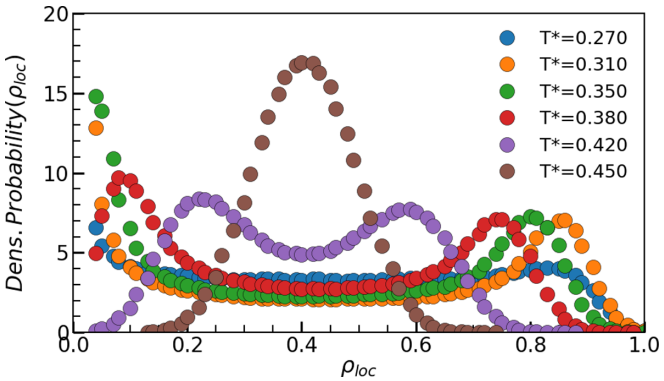

FIG. 2. Local density probability for a patchy colloidal system with $n = 3$ and $\chi = 0.6$ with a reduced bulk density $\rho^* = 0.4$ and an attraction range $\lambda = 1.2$ for different reduced temperatures. The brown circles correspond to a state above the binodal.

C. Calculation of the phase diagram of patchy colloidal systems

In the literature, the calculation of the phase diagram of patchy colloids has been carried out using a perturbation theory [41], as well as computer simulations [42,43]. The most common simulation technique to study the phase equilibrium of particles with short-ranged interactions is the Gibbs-ensemble method [44] along with the well-known parallel tempering technique [45]. We are aware of the complications of using the Gibbs ensemble method for particles with short-ranged attractions, we expect the complications to increase for particles with nonisotropic interactions. Then, we here use a different approach based on the use of an NVT simulation and the calculation of the local density across the simulation box [46].

Once the simulation reaches thermodynamic equilibrium, random points are generated inside the simulation box, which are at the center of spheres with an arbitrary radius, usually five times smaller than the box length. The number of particles inside those spheres are counted and the local density is calculated as $\rho_{\text{loc}} = N_s/v_s$, where N_s is the number of particles inside the sphere with volume v_s. During the simulation, we compute a density histogram, which behaves as follows: for a system above the coexistence region the distribution is centered around the reduced bulk density, ρ^*; for a phase separated system, the histogram exhibits two peaks, one at the gas and the other at the liquid density [46]. Figure 2 displays the histogram for colloidal particles with three patches; the critical temperature for this system is 0.425.

D. Determination of the structural and dynamical properties of patchy particles

To determine the structural properties of a patchy colloidal system, we have computed some structural quantities. (1) The average number of bonds per particle, also called the mean coordination number, $\langle n_b \rangle$. The bonding between particles is defined without ambiguity; particles that lie within the attractive part of the Kern-Frenkel potential are bonded, then $\langle n_b \rangle$ is proportional to the average energy per particle. (2) The radial distribution function, $g(r)$; despite this quantity does not provide information about the orientation of the particles,

it is useful to measure the spatial distribution of particles inside the volume and to estimate, in a rough way, how similar, structurally speaking, are two colloidal systems. (3) The cluster size distribution, Pr(s), is related to the probability of finding a cluster with s-particles. This is obtained by listing connected particles by direct bonds and after that comparing recursively element by element of the list, erasing and adding new elements until complete the list of particles connected via indirect bonds. A similar technique can be done using a bond matrix method [47]. From that distribution, one can compute the average cluster size as

$$S = \frac{\sum_s s^2 \overline{n}(s)}{\sum_s s\overline{n}(s)}, \tag{6}$$

where s is the number of particles in a given cluster and $\overline{n}(s)$ is the mean number of cluster of size s [47].

The percolation threshold could be defined in different but equivalent ways, however, the results obtained via different methods do not agree because they are highly dependent on the system size. Instead, we calculate the percolation threshold as it is done by Bug *et al.* [48]. At a given reduced temperature, we search for the density at which the probability of finding at least one percolating cluster in the system is $E_p = 0.5$. This method is a good approximation for determining the percolation threshold, which should be located at the inflexion point of the $E_p(\rho)$ curve [49].

The transport properties of patchy particles are accounted for in terms of the so-called mean-square displacement, $\Delta\vec{r}^2(t) = \langle(\vec{r}(t) - \vec{r}(0))^2\rangle$, and the intermediate scattering function, $F_{\text{self}}(q,t) = \langle \exp[-i\vec{q}\cdot\Delta\vec{r}(t)]\rangle$, where the brackets denote an ensemble average and $\vec{q}$ is the wave vector [50]. We have chosen $q^* \equiv q\sigma = 6.18$; this value is close to the characteristic length given by the main peak of the static structure factor. Both quantities are obtained by using the so-called dynamic Monte Carlo technique, which will be explicitly discussed further below.

E. Single-bond condition analysis

As we mentioned in the Introduction, the single-bond condition between patchy particles is usually imposed with the aim of comparing the simulation results with theoretical predictions based on the Wertheim perturbation theory [28]. In this contribution, we have relaxed that condition. However, one would ask whether such a condition limits the number of bonds that each particle can form. This is a crucial aspect since our main conjecture is that patchy particles should reach a coordination number equal to 2.4 at the gel state.

To check the number of bonds per patchy particle within the single-bond condition, we consider the case $n = 18$ and $\lambda = 1.1$ because a particle with a large amount of patches has a relatively big coverage and satisfies the single-bond condition, simultaneously. The single-bond condition is reached if the patch aperture δ obeys the following inequality [51],

$$\sin\delta \leqslant \frac{1}{2\lambda}. \tag{7}$$

According to the previous expression, the maximum aperture angle that corresponds to $\lambda = 1.1$ is $\delta_{\max} = 0.4719$, which leads to the maximum coverage $\chi_{\max} = 0.9836$. For this case, patchy particles become almost isotropic and, in fact, the patches overlap withe their neighbors. A coverage that still obeys the inequality, avoids the overlapping and conserves the anisotropy is $\chi = 0.26053$. The latter is considered within Monte Carlo simulations that guarantee the single-bond condition for $n = 18$.

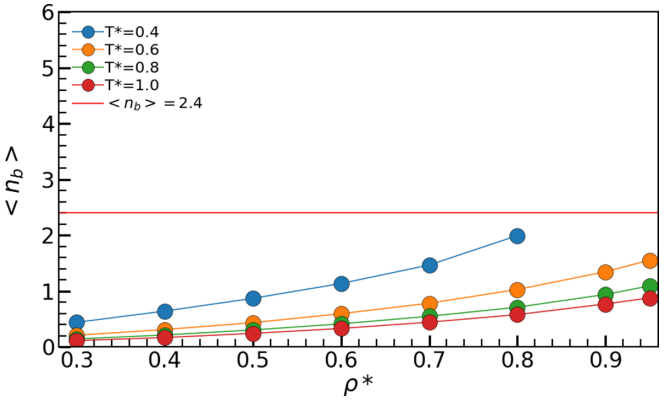

FIG. 3. Coordination number as a function of the bulk reduced density at different temperatures for a colloidal system with $n = 18$ patches. The red horizontal line represents the average number of bonds per particle equal to 2.4.

In Fig. 3, the coordination number as a function of the reduced bulk density is displayed. From the figure, one can observe that at high and intermediate temperatures, patchy colloidal systems with low coverages cannot attain the condition $\langle n_b\rangle = 2.4$ (horizontal line). Thus, the single-bond condition does not guarantee the enough number of bonds per particle required to reach the rigidity percolation state. At the lowest temperature,, $T^* = 0.4$, and highest concentrations, $\rho^* > 0.8$, here considered the simulations did not reach thermodynamic equilibrium (those states were not included in the corresponding isotherm). Nevertheless, at low temperatures and high densities, one would expect a kind of attractive-driven glass transition, as discussed recently in Ref. [52], which is a topic out of the main goal of this contribution. Hence, from this analysis, the single-bond condition case is not longer considered in this work.

Table I shows the maximum coverage for each patchy colloidal system ($n = 18$ omitted) that satisfies the single-bond condition. As can be noticed, all of them have smaller coverages than the ones studied in this contribution.

TABLE I. Maximum coverage that obeys the single-bond condition for the different values of the attractive range, λ, and number of patches, n.

n	$\chi_{\max}(\lambda = 1.1, \delta_{\max} = 0.4719)$	$\chi_{\max}(\lambda = 1.2, \delta_{\max} = 0.4298)$
1	0.0546	0.0455
2	0.1093	0.0905
3	0.1639	0.1364
4	0.2186	0.1819

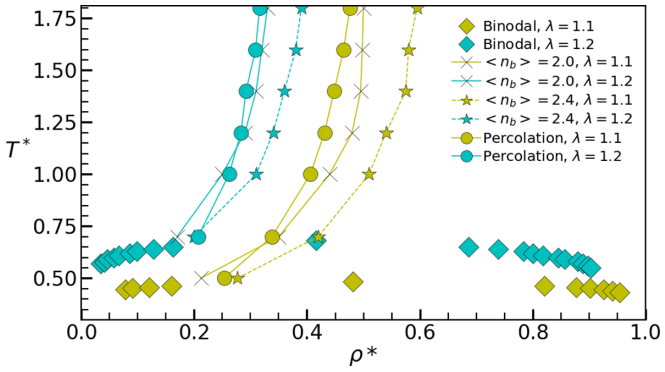

FIG. 4. Phase diagram for isotropic square-wells with attraction ranges $\lambda = 1.1$ (yellow) and $\lambda = 1.2$ (cyan) [46]. Also, the connectivity percolation threshold and the curves where the following conditions $\langle n_b \rangle = 2.0$ and $\langle n_b \rangle = 2.4$ were fulfilled are plotted.

III. PHASE DIAGRAM OF PATCHY COLLOIDS

In previous works, we have pointed out the importance of the estimation of the binodal as a good indicator of those thermodynamic states where the formation of a cluster fluid seems to occur [53]; this includes colloidal systems where the particles interact with either isotropic short-ranged attractions or competing interactions. Also, two of us have found that gelation is preceded by the rigidity percolation [35] at conditions above the binodal line, i.e., homogeneous gelation takes place. Then, finding the binodal of the system, or the one of a reference system, is useful to locate the thermodynamic states that might be associated with clustering and ultimately with the homogeneous gel formation.

The binodal curve, as well as the connectivity percolation threshold, for systems with isotropic short-ranged attractions, $\lambda = 1.1$ and 1.2, are shown in Fig. 4. Those curves are considered as our reference to investigate both the structure and the gel formation in patchy colloidal systems. In particular, we focus our attention on thermodynamic states above the binodal of the reference system because the coexistence curves of patchy colloids are typically below the isotropic one [10]. We calculated the binodals for some patchy colloidal systems (data not shown), but in most cases this was not the case because this represents a high computational cost and besides those calculations are also out of the scope of this work.

In Fig. 4, the thermodynamic states identified by the condition $\langle n_b \rangle = 2.0$ are displayed along with the connectivity percolation threshold. As it can be noticed, particularly for the cases with an attraction range $\lambda = 1.2$, the curves associated with those states are close each other. Then, one can consider that both conditions give rise to the same thermodynamic states. A similar result was also reported in Ref. [11] for shorter attractive ranges. However, it is important to point out that the thermodynamic states where the condition $\langle n_b \rangle = 2.4$ is satisfied are always located at densities above the percolation threshold for both interaction ranges. We have also found that such states correspond to $E_p \approx 1.0$ (data not shown).

As mentioned in the previous section, we have used the local density distribution method to roughly estimate the critical temperature for particles with $n = 2$, 3, and 4 patches: all of them with $\chi = 0.6$ and range $\lambda = 1.2$; for smaller coverages the method does not work correctly. The resulting critical temperatures are $T^*_{n=4} \approx 0.43$, $T^*_{n=3} \approx 0.425$, and $T^*_{n=2} \approx 0.39$. We expect a lower temperature for the one-patch system, however, we could not compute accurately the critical temperature for this case. We only provide an estimation of the critical temperature due to the difficulty to precisely calculate the coexistence curve in patchy colloidal systems [54]. The problem resides in the enormous amount of time necessary to reach thermal equilibrium and the fact that many particles are needed to have enough resolution of the local densities distribution to distinguish the maxima associated to each phase. From now on, we only present results for those thermodynamic states above the critical temperature.

IV. RIGIDITY PERCOLATION IN PATCHY COLLOIDAL SYSTEMS

A gel state is usually characterized by the formation of a percolating network [7]. However, connectivity percolation represent thermodynamic states that do not support mechanical stresses. In a previous work, two of us found that a percolating colloidal system composed of adhesive particles in which the average coordination number is $\langle n_b \rangle$ =2.4 corresponds to gel states identified in experiments [23]. The condition given by $\langle n_b \rangle$ =2.4 is associated to a kind of percolation state known as rigidity percolation (RP) [11]. Then, the onset of gelation might be linked to RP. Interestingly, new experimental evidence reported in Ref. [14] shows that states at RP also corresponds to gel states in systems made of rodlike particles interacting with very short-range attractions. It is worth mentioning that originally the RP accounts for the glass transition in molecular systems whose interactions (mainly covalent) are anisotropic in nature [35], however, it is interesting that such a mechanism also precedes gelation in the colloidal domain. In this work, we assume that RP also applies for systems with highly directional interactions to estimate the location of the boundary of gelation in patchy colloids.

To find the thermodynamic states where rigidity percolation occurs, we first find the connectivity percolation threshold, ρ_p, at a given T^*. After that, we measure the bond distribution, $P(n_b)$, at densities above ρ_p. From this distribution, we compute the coordination number $\langle n_b \rangle$. For SW-like particles, it is known that the energy per particle is given by $u \equiv U/N = -\frac{1}{2}\langle n_b \rangle \epsilon$, which is a quantity that can be straightforwardly computed in any Monte Carlo computer simulation. For a constant T^*, we obtain $\langle n_b \rangle$ for different densities around ρ_p. Then, we fit $\langle n_b \rangle$ using a quadratic function. The density at which rigidity percolation occurs is thus reached when the condition $\langle n_b \rangle = 2.4$ is satisfied. Hence, from now on, we identify the condition $\langle n_b \rangle = 2.4$ with RP and it will also be our criterion to define the "mean-field rigidity boundary." Although this is a pure heuristic criterion, we will show further below that it is indeed an excellent approximation to identify those thermodynamic states associated to RP.

In Fig. 5, the thermodynamic states linked to rigidity percolation for a system of patchy particles with one and four patches and attraction range $\lambda = 1.1$ are plotted; different χ values are displayed. The results indicate that for the same interaction range and same coverage the mean-field rigidity curve has, more or less, the same shape regardless the number

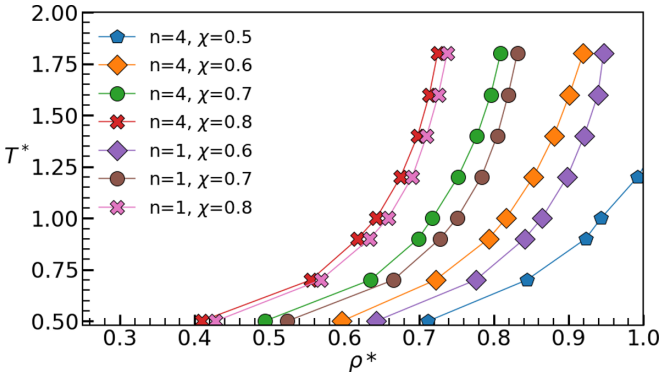

FIG. 5. Mean-field rigidity or gel-like curves for patchy particles with $n = 1$ and 4 patches and for different values of coverage. The attraction range is $\lambda = 1.1$. Only thermodynamic states above the binodals are plotted.

of patches. Furthermore, the effect of increasing the number of patches is to shift slightly the curves to lower densities.

The above results are of utmost importance. One of the consequences is that the gel-like state is suppressed at certain coverage. This was observed for $\chi \lessapprox 0.5$, since the condition $\langle n_b \rangle = 2.4$ cannot been attained for both attractive ranges. Hence, there is a critical coverage that indicates that for coverages below it one cannot find gel-like states. This behavior is associated to the fact that a minimum coverage is needed to guarantee the formation, on average, of at least 2.4 bonds per particle. This is an important aspect that could be applied for the technological design of new materials that, according to the potential application, one would like to avoid or promote the onset of gelation by simply tuning the coverage value.

Mean-field rigidity or gel-like curves are displayed in Fig. 6 in terms of the reduced bulk density and the second virial coefficient for the cases $\chi = 0.6$ and 0.7, for particles with one to four patches and for attractions ranges $\lambda = 1.1$ and 1.2. We observe the same behavior for $\chi = 0.5$ and 0.8 (data not shown). It can be noticed that the effect of decreasing the coverage is to shift the boundary of gelation at higher densities. This means that the gel density for the same temperature is larger, as can be seen in the snapshots of Fig. 7. In the latter, we have selected the case with $n = 4$ patches because it is the patchy colloidal system with less degree of anisotropy in the interaction and the mean-field rigidity curve is reached at lower densities. Furthermore, this case allows us to observe the percolation cluster. It is important to stress out that for high coverage values, χ is the quantity that basically dictates the general behavior of the gel boundary. In the case of small coverages, the number of patches and their arrangement should be more relevant.

The representation of the gel-like states given in Fig. 5 makes evident that for a given attraction range the boundary of gelation is basically dependent on the coverage, however, the representation illustrated in Fig. 6 highlights the fact that for patchy particles the gelation curves seem to collapse onto a kind of a universal curve that slightly depends on the attraction range. Then, the idea that the onset of gelation in patchy colloids only depends on the second virial coefficient provides an interesting extension of the so-called extended

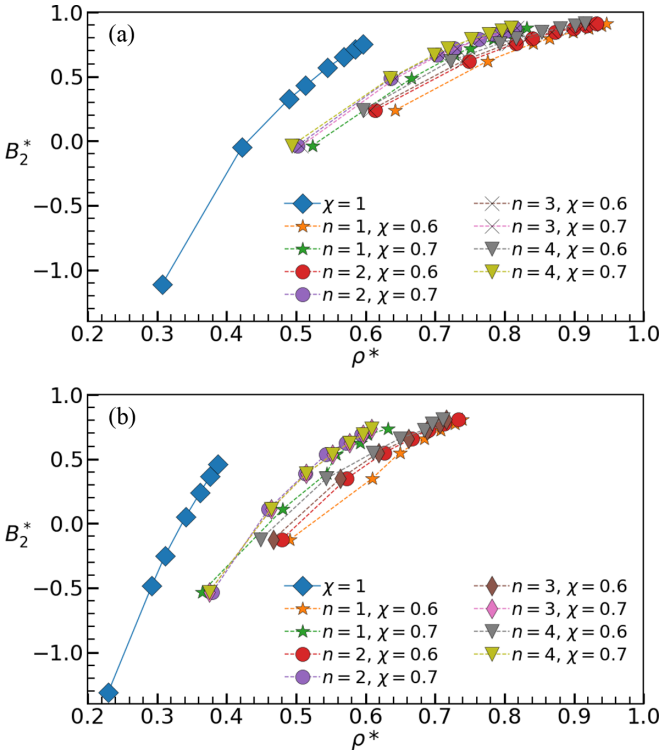

FIG. 6. Mean-field rigidity or gel-like curves in the B_2^* vs ρ^* state diagram for particles with attraction range (a) $\lambda = 1.1$ and (b) $\lambda = 1.2$, and for different number of patches and coverages. The blue diamonds represent the $\langle n_b \rangle = 2.4$ curve for the isotropic system at the corresponding attractive range.

law of corresponding states (ELCS) [55]; however, a deeper and systematic study to prove this point is still needed. An important aspect to remark is that Kern and Frenkel [44] showed that the ELCS is not fulfilled for the binodals of patchy colloids, but it seems to be the case for the gelation curves.

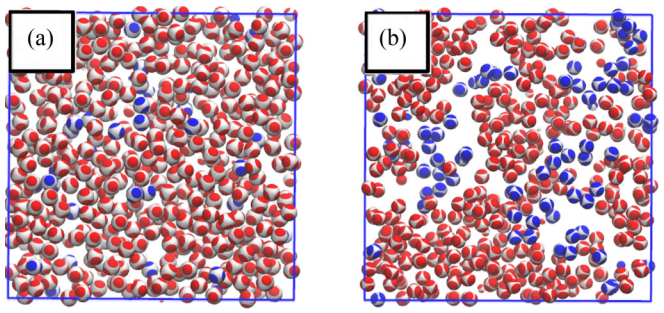

FIG. 7. Snapshot of two different patchy colloidal systems with $\lambda = 1.2$, $n = 4$ and $T^* = 0.9$. (a) $\chi = 0.5$ and $\rho^* = 0.584$. (b) $\chi = 0.7$ and $\rho^* = 0.374$. The red patch particles belong to the percolating cluster and the blue ones are from different clusters. We only show particles near the frontal face of the cube with the aim of appreciating better the difference between both systems.

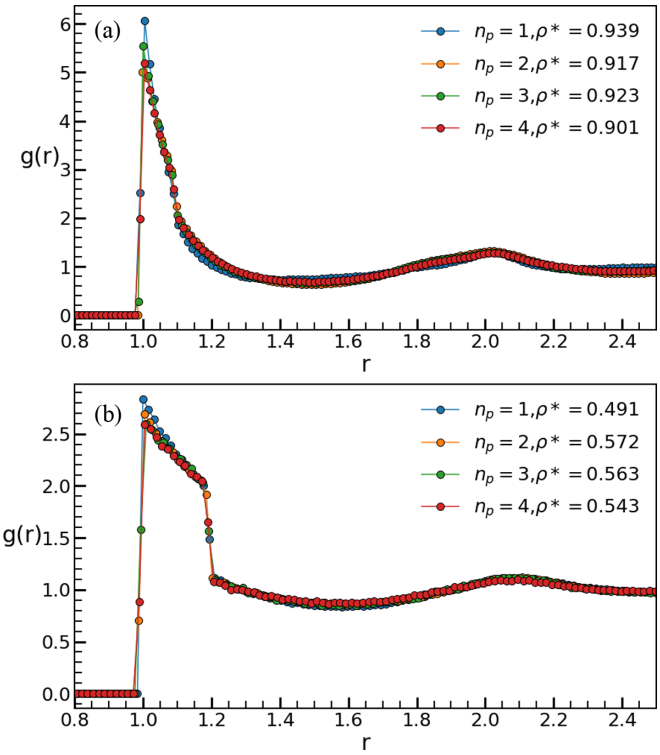

FIG. 8. Radial distribution functions for patchy colloidal systems at the gel-like states reported in Fig. 6 for different number of patches ($n = 1, 2, 3,$ and 4) and same coverage $\chi = 0.6$. (a) $\lambda = 1.1$ and $T^* = 0.6$. (b) $\lambda = 1.2$ and $T^* = 0.8$.

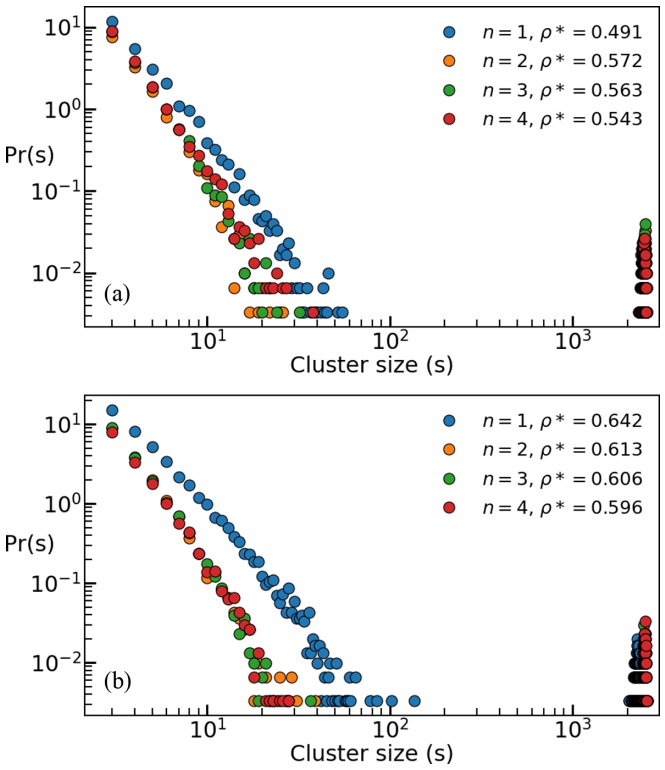

FIG. 9. Cluster size distribution along some of the gel-like states displayed in Fig. 6 for $\chi = 0.6$. (a) $\lambda = 1.2$, $T^* = 0.8$. (b) $\lambda = 1.1$, $T^* = 0.5$.

V. STRUCTURE AND CLUSTER SIZE DISTRIBUTION AT THE GEL-LIKE STATES

We have determined the gel-like states in patchy colloids using empirically the rigidity percolation criterion. However, one can also learn on the rich structural scenario that emerges along those particular states. To this end, we have calculated the radial distribution function and the cluster size distribution to highlight the structural differences and similarities on the gel-like states for particles with different coverage fractions and number of patches.

We then simulate patchy colloidal systems with $N = 3375$ particles. We have found that those systems have a radial distribution function very similar regardless the number or the position of the patches when compared at the same temperature, as it is explicitly shown in Fig. 8. The results are plotted for both attraction ranges. The fact that the structure, at a given attraction range, is identical for each isotherm regardless the number of patches is consistent with the fact that along those gel-like states the B_2^* is the same, which would imply isostructurality.

In Fig. 9, we have selected representative cases for both attractive ranges with the main goal of highlighting the fact that all states over the mean-field rigidity curves have at least one cluster that spans the entire volume in all directions. Furthermore, one can observe the same behavior or trend for the cluster size distribution, regardless the range of the attraction, however, there exist differences attributable to the latter; the biggest cluster for the lowest number of patches is smaller than the other cases. To better understand this behavior, one has to consider that a system that has a big cluster which contains most of the particles will have other small aggregates or even a lot of individual particles that do not belong to the biggest aggregate, meaning that the left part of the distribution is near to one and the last peak near the total number of particles in the system. It is worth mentioning that the deviations for those systems with a single patch are much bigger that the others because it is considered the most anisotropic case. Such deviations tell us an important aspect about the angular dependence that is more or less obvious, namely, if the number of patches is too high, the orientation dependence will eventually decrease.

In the following section, we will analyze whether the resulting percolating cluster is rigid, leading to mechanical stability, and mainly to corroborate that the heuristic criterion given by $\langle n_b \rangle = 2.4$, which is linked to mechanical transitions in molecular materials [22], also holds for patchy colloidal systems.

VI. BOND-BENDING NETWORK ANALYSIS IN PATCHY COLLOIDS

So far, we have identified the gel-like states in patchy colloidal systems with those thermodynamic states where the condition $\langle n_b \rangle = 2.4$ is fulfilled. Such a condition is associated to the so-called rigidity percolation in network-forming materials [22]. This is an instantaneous static property that cannot provide any physical information on the particle dynamics. In rheological terms, it tells us whether $G' > G''$ for

infinite frequency. However, as we pointed out above, recent experimental colloidal gel states were identified with the onset of a rigid and mechanically stable network that also satisfies the previous condition [11]. Nonetheless, the proper calculation of the states where RP occurs should allow us to either discard or corroborate our conjecture. Thus, in this section, we introduce the so-called bond-bending analysis, implemented for the case of patchy colloids, to account for the formation of rigid networks and, mainly, to assess the accuracy of the condition $\langle n_b \rangle = 2.4$ even for colloids interacting with highly directional potentials.

We have implemented the Chubynsky and Thorpe analysis where the well-known pebble game, based on the technique proposed by Jacobs [56], is adapted to study a particular type of three-dimensional networks called bond-bending networks [24]. In a bond-bending network, the sites are exclusively bonded to their first neighbors and angularly constrained with their second neighbors [57]. These conditions are met by the colloidal systems with $n = 3$ and $n = 4$ patches. The $n = 1$ and $n = 2$ cases allow the formation of three particles bonded with each other, thus breaking the bond-bending condition.

Several quantities depend only on the spatial distribution of particles. One of them is the number of floppy modes, which can be defined as the linearly independent infinitesimal movements that do not deform a constriction, and because that, do not cost energy. The number of floppy modes is directly related with the rigidity of the cluster. Rigidity percolation occurs when the number of floppy modes tends to zero [24].

The "pebble game" method is a combinatorial algorithm based on the Lamman theorem [58], which establishes that a graph with N vertices and E edges is minimally rigid if there is no subgraph with more than $2N - 3$ edges. This theorem is exact only in 2D and not generalizable to 3D [24]. However, this method is applicable to three dimensional bond-bending networks, where the equivalent conjeture is that a graph in 3D is minimally rigid if there is no subgraph with more than $3N - 6$ edges. The pebble game for bond-bending networks has been used to identify rigidity and flexibility substructures in proteins [59]. As far as we know, this might be the first time that such a scheme is applied to study the rigidity of networks formed by patchy particles.

The algorithm works as follows: Starting with an empty network and assigning 3 pebbles to N vertices (particles), equivalent to 3 degrees of freedom. One adds one bond to the network and proceeds to test its independence or redundancy. A bond is independent if it is possible to free an extra pebble from the first neighbor from one side. Then, the bond is covered by one free pebble available from either particle attached to the bond. As we add bonds to the graph, free pebbles are used to cover them. A redundant bond occurs when it is not possible to free a single pebble of the subnetwork and all subnetworks are declared minimally rigid and the bond is not covered. This process is repeated until there are no more bonds to add to the network. At the end of the analysis, the remaining free pebbles represent the floppy modes associated to the network.

In Fig. 10, the analysis of the rigidity of the percolating cluster for the colloidal system reported in Fig. 5 with $n = 4$ patches and $\lambda = 1.1$ is shown. For each curve, error bars were

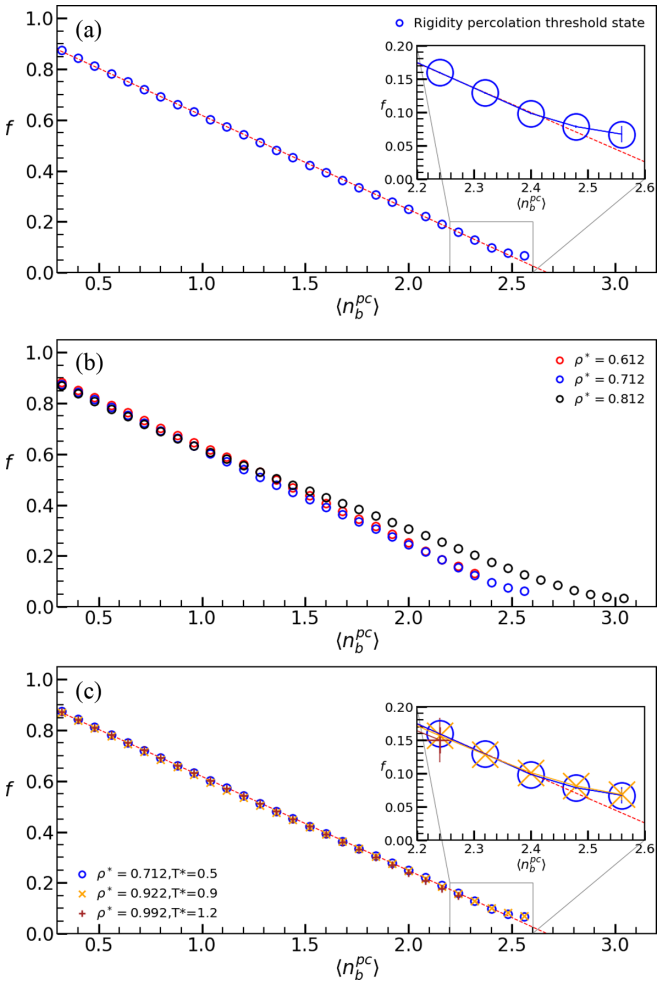

FIG. 10. Fraction of floppy modes f as a function of the mean coordination of the percolating cluster $\langle n_b^{pc} \rangle$ for the colloidal systems with $n = 4$ patches and $\lambda = 1.1$. (a) Empty blue circles belong to the thermodynamic state $\rho^* = 0.712$, $T^* = 0.5$, which lies at the RP curve reported in Fig. 5. (b) Three curves at different densities for the same temperature $T^* = 0.5$; lower density system (empty red diamonds), higher density system (black empty diamonds) and the system where RP occurs (empty blue circles). (c) Number of floppy modes for those thermodynamic states along the RP curve (see Fig. 5). Insets show a close up of the region where the fraction of floppy modes breaks its linear behavior; this occurs around $\langle n_b^{pc} \rangle = 2.4$ and the solid line is just a guide for the eye. Error bars are smaller than the symbol size. The results were obtained by averaging over 83 different clusters.

calculated, but they are smaller than the symbol size. It is important to note that $\langle n_b \rangle$ is the mean coordination number, whereas $\langle n_b^{pc} \rangle$ is the mean coordination of the percolating cluster only, which depends on the attractive range, number of patches and the coverage. Almost every percolating cluster contains over 80% of the particles of the whole system.

Figure 10(a) makes evident that our assumption about the localization of the rigidity percolation curve is right, namely, the rigidity percolation starts when the number of floppy modes curve deviates from the linear behavior [24]; this occurs approximately at $\langle n_b^{pc} \rangle \sim 2.4$. This result is complemented with the analysis reported in Fig. 10(b), which shows a

comparison between states before and after the RP threshold; the red empty diamond curve preserves linear behavior because is at the left of the RP threshold. For all thermodynamic states along the RP curve (shown in Fig. 5), the bond-bending analysis displayed in Fig. 10(c) exhibits a very similar behavior. All curves are near the loss of linearity, meaning that all of them are in the RP threshold, pointing out the fact that the criterion $\langle n_b \rangle = 2.4$ describes correctly the rigidity percolation transition even for patchy colloidal systems.

VII. PARTICLE DYNAMICS IN THE REGION NEAR THE RIGIDITY PERCOLATION THRESHOLD

A viscoelastic material, such as a gel, behaves as a solid at times shorter than its relaxation time, although stresses are able to relax at long time due to the dynamic nature of the physical bonds between particles. Thus, one intriguing aspect of colloidal gels is the nature of the particle dynamics and its connection with the formation of rigid or mechanically stable structures, mainly because bonds are being formed and broken continuously. Furthermore, one can also think that due to the nonequilibrium nature of such thermodynamic states, the transport behavior should resemble the features observed in the classical glassy dynamics [60]. Experimental evidence [18] shows that the latter scenario is not the general physical picture of gel dynamics and recent molecular dynamics simulation results [52] point out the fact that even at higher densities and lower temperatures that the ones here considered, i.e., close to glassy states, the long-time dynamics of patchy colloids behave normal, i.e., as in the fluid phase. However, since we have already identified the gel-like states, it would be advantageous to study the particle dynamics along the rigidity percolation curve.

The colloid dynamics is calculated using the dynamic Monte Carlo (DMC) technique for particles with orientational degrees of freedom [61,62]. This is a good approximation to represent the diffusive dynamics, i.e., within the Brownian regime, in the case of a very small Monte Carlo displacement δl. The connection between the real time and the Monte Carlo displacement can be established using the following expression [63]:

$$\delta t_t = \frac{A_t \delta l^2}{6 D_t^0}, \tag{8}$$

where δt_t is the Brownian time translational interval per MC cycle, A_t is the average translational acceptance and D_t^0 is the free-particle diffusion coefficient [50]. Also, there is a relation between the angular displacement and the real time,

$$\delta t_r = \frac{A_r \delta \theta^2}{18 D_r^0}, \tag{9}$$

with δt_r being the real time rotational interval per MC cycle, $\delta\theta$ is the angular displacement, A_r is the average rotational acceptance and D_r^0 is the rotational free-particle diffusion coefficient [50]. Both rotational and transnational diffusion coefficients are related through the Stokes-Einstein relation [61], leading to the expression $D_r^0 \sigma^2 = 3 D_t^0$ [64]. The times given by Eqs. (8) and (9) must be equal. This allows one to express δt_r in terms of D_r^0 and to obtain the following relationship:

$$\frac{\delta l}{\delta \theta} = \frac{\sigma}{3}\sqrt{\frac{A_r}{A_t}}. \tag{10}$$

By fixing δl and A_t, $\delta\theta$ and A_t are computed iteratively.

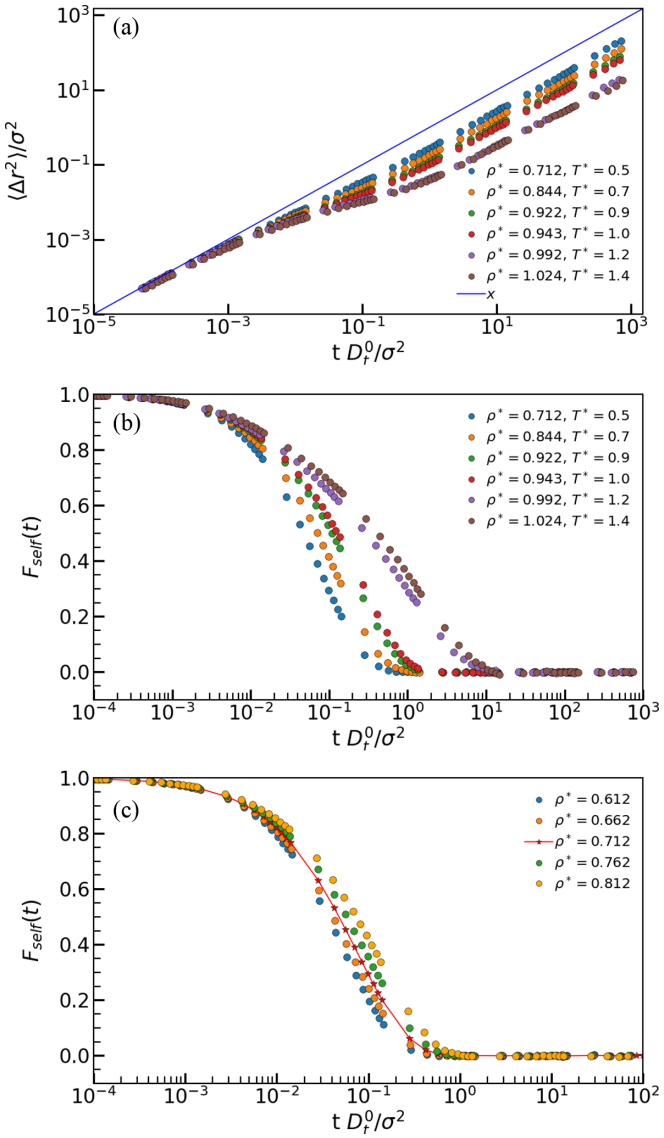

FIG. 11. (a) Mean-square displacement and (b) intermediate scattering function with $q^* = 6.18$ for those thermodynamic states along the mean-field rigidity curve for $n = 4$ patches, $\chi = 0.5$ and $\lambda = 1.1$ reported in Fig. 5. (c) Intermediate scattering functions in the neighborhood of $\rho^* = 0.712$, $T^* = 0.5$ (the thermodynamic density at which RP occurs). All dynamic Monte Carlo simulations were carried out using $\delta l = 0.01$, which in Brownian time corresponds approximately to $\sim 10^{-5}$.

The mean-square displacement (MSD) displayed in Fig. 11(a) corresponds to the gel-like states presented in Fig. 5. As seen in the figure, the particle dynamics exhibits the typical diffusive dynamics observed in fluid-like states at all time scales, i.e., at long times, it does not show evidence of a glassy-like dynamics and the corresponding long-time self-diffusion coefficient decreases with the density (data not

shown). Figure 11(b) displays the intermediate scattering function along the RP curve. The features seen in this case are also typical of a fluid-like state; the curve decays in all cases and its relaxation time increases with the particle density. In Fig. 11(c), one can note that the particle dynamics does not exhibit a particular transition or anomaly when the RP threshold is crossed. This is clearly related with the fact that we are dealing with homogeneous gels, which occur at intermediate densities and above the critical temperature [11]. Of course, one can appreciate that the particle motion becomes slightly slow at intermediate times (mainly at higher densities), but the long-time self-diffusion does not exhibit any evidence of a kind of glassy dynamics, i.e., the MSD does not reach the standard plateau linked to dynamical arrest [52]. As mentioned above, these results agree with recent results of glass-former patchy particles [52], where the dynamics of particles with 8 and 12 patches interacting with short-range attractive forces was reported above the critical temperature; authors found that the glassy dynamics is only observed at extreme thermodynamic conditions, namely, high densities and low temperatures.

VIII. CONCLUDING REMARKS AND PERSPECTIVES

By means of Monte Carlo computer simulations, we have studied the onset of gelation in patchy particles interacting with highly directional and short range attractive potentials by systematically varying the coverage χ, the number of patches, n, and the attractive range, λ. We mainly located those thermodynamic states associated with gelation by using the criterion provided by He and Thorpe for rigidity percolation, i.e., the coordination number at the RP threshold takes the value $\langle n_b \rangle = 2.4$. This assumption is strongly supported by experimental evidence [14]. However, by computing the number of floppy modes of the resulting percolating clusters, we concluded the validity of the aforementioned criterion at least in the cases with $n = 3$ and $n = 4$ patches. A different analysis is required to study the rigidity of the percolating clusters in the cases of $n = 1$ and $n = 2$ patches.

Our analysis also pointed out several important and interesting results. For example, we found that not all coverages lead to the formation of a gel; there is a minimum coverage needed to form, on average, 2.4 bonds. Roughly speaking, systems with a coverage bigger than $\chi \approx 0.5$ can reach a gel-like state. This is an important technological aspect that should be potentially used to facilitate or inhibit the formation of gels in functionalized particles.

We also observed that for high coverages, the gel-like states were mainly dominated by χ, regardless the way in which patches are arranged on the particle surface. The opposite was observed at lower coverages. However, we noticed that all mean-field rigidity curves followed a kind of universal behavior when they were particularly plotted in terms of the reduced second virial coefficient. These gel-like states were calculated above the binodals, which means that they form homogeneous gels not associated with an interruption of the spinodal decomposition. It is important to highlight that our exploration can be used to predict the conditions at which gelation occurs as function of the coverage.

From the structural analysis along the gel-like states, we observed isostructurality and the appearance of clusters that span the entire volume; however, the cluster size distribution showed that the percolating cluster is bigger for the cases with higher valence or number patches. As mentioned above, the bond-bending analysis provided enough evidence that such percolating clusters are mechanically stable and rigid networks; one of the crucial signatures of colloidal gelation. The calculation of both the mean-square displacement and self-intermediate scattering function showed that the particle dynamics at those thermodynamic states identified as potential candidates of gel states became slow, but not so slow enough as in the glassy dynamics scenario. The transport behavior of patchy particles that are able to form physical gels at intermediate densities and above the phase coexistence has not been studied in detail yet, which undoubtedly constitutes a fascinating problem to be solved.

Last, but not least, we should stress out that we have established rigidity percolation mechanism as the potential precursor of gelation in patchy colloidal systems. This helped us to identify the states where gelation might eventually occur. Of course, our contribution naturally extends the previous experimental observations performed in adhesive (spherical and nonspherical) colloidal dispersions. With this information at hand, we can systematically study and characterize the mechanical and viscoelastic properties of gels made up of particles interacting with orientational dependent potentials. Work along this direction is currently in progress.

ACKNOWLEDGMENTS

R.C.-P. acknowledges the financial support provided by the Consejo Nacional de Ciencia y Tecnología (CONACYT, Mexico) through Grants No. 237425 and No. 287067. N.E.V.-P. also acknowledges financial support from CONACyT through the program Retenciones 2019-1. and to Autonomous University of Chiapas Project No. 01/FYM/RPR/278/20.

[1] R. Castañeda-Priego, Colloidal soft matter physics, Rev. Mex. Fis. **67**, 050101 (2021).

[2] Z. Wang, Z. Wang, J. Li, S. T. H. Cheung, C. Tian, S.-H. Kim, G.-R. Yi, E. Ducrot, and Y. Wang, Active patchy colloids with shape-tunable dynamics, J. Am. Chem. Soc. **141**, 14853 (2019).

[3] Y. Lu, E. Zhang, J. Yang, and Z. Cao, Strategies to improve micelle stability for drug delivery, Nano Res. **11**, 4985 (2018).

[4] S. Schnittger and M. Sinha, The materials science of cosmetics, MRS Bull. **32**, 760 (2007).

[5] N. E. Valadez-Pérez, Y. Liu, and R. Castañeda-Priego, Reversible Aggregation and Colloidal Cluster Morphology: The

Importance of the Extended Law of Corresponding States, Phys. Rev. Lett. **120**, 248004 (2018).
[6] M. F. Thorpe, D. J. Jacobs, M. V. Chubynsky, and J. C. Phillips, Self-organization in network glasses, J. Non-Cryst. Solids **266-269**, 859 (2000).
[7] E. Zaccarelli, Colloidal gels: equilibrium and non-equilibrium routes, J. Phys.: Condens. Matter **19**, 323101 (2007).
[8] P. J. Lu, E. Zaccarelli, F. Ciulla, A. B. Schofield, F. Sciortino, and D. A. Weitz, Gelation of particles with short-range attraction, Nature (London) **453**, 499 (2008).
[9] H. Firoozmand and D. Rousseau, Microbial cells as colloidal particles: Pickering oil-in-water emulsions stabilized by bacteria and yeast, Food Research International **81**, 66 (2016).
[10] S. Griffiths, F. Turci, and C. P. Royall, Local structure of percolating gels at very low volume fractions, J. Chem. Phys. **146**, 014905 (2017).
[11] N. E. Valadez-Pérez, Y. Liu, A. P. R. Eberle, N. J. Wagner, and R. Castañeda-Priego, Dynamical arrest in adhesive hard-sphere dispersions driven by rigidity percolation, Phys. Rev. E **88**, 060302(R) (2013).
[12] M. Kohl, R. F. Capellmann, M. Laurati, S. U. Egelhaaf, and M. Schmiedeberg, Directed percolation identified as equilibrium pre-transition towards non-equilibrium arrested gel states, Nat. Commun. **7**, 11817 (2016).
[13] H. Tsurusawa, M. Leocmach, J. Russo, and H. Tanaka, Direct link between mechanical stability in gels and percolation of isostatic particles, Sci. Adv. **5**, eaav6090 (2019).
[14] R. P. Murphy, H. W. Hatch, N. A. Mahynski, V. K. Shen, and N. J. Wagner, Dynamic arrest of adhesive hard rod dispersions, Soft Matter **16**, 1279 (2020).
[15] E. D. Gado, A. Fierro, L. de Arcangelis, and A. Coniglio, Slow dynamics in gelation phenomena: From chemical gels to colloidal glasses, Phys. Rev. E **69**, 051103 (2004).
[16] H. H. Winter and F. Chambon, Analysis of linear viscoelasticity of a crosslinking polymer at the gel point, J. Rheol. **30**, 367 (1986).
[17] L. C. Hsiao, M. J. Solomon, K. A. Whitaker, and E. M. Furst, A model colloidal gel for coordinated measurements of force, structure, and rheology, J. Rheol. **58**, 1485 (2014).
[18] J. H. Cho, R. Cerbino, and I. Bischofberger, Emergence of Multiscale Dynamics in Colloidal Gels, Phys. Rev. Lett. **124**, 088005 (2020).
[19] S. Corezzi, L. Palmieri, J. M. Kenny, and D. Fioretto, Clustering, glass transition and gelation in a reactive fluid, J. Phys.: Condens. Matter **17**, S3557 (2005).
[20] A. P. R. Eberle, N. J. Wagner, and R. Castañeda-Priego, Dynamical Arrest Transition in Nanoparticle Dispersions with Short-Range Interactions, Phys. Rev. Lett. **106**, 105704 (2011).
[21] A. Coniglio, L. De Arcangelis, E. D. Gado, A. Fierro, and N. Sator, Percolation, gelation and dynamical behaviour in colloids, J. Phys.: Condens. Matter **16**, S4831 (2004).
[22] H. He and M. F. Thorpe, Elastic Properties of Glasses, Phys. Rev. Lett. **54**, 2107 (1985).
[23] A. P. R. Eberle, R. Castañeda-Priego, J. M. Kim, and N. J. Wagner, Dynamical arrest, percolation, gelation, and glass formation in model nanoparticle dispersions with thermoreversible adhesive interactions, Langmuir **28**, 1866 (2012).
[24] M. V. Chubynsky and M. F. Thorpe, Algorithms for three-dimensional rigidity analysis and a first-order percolation transition, Phys. Rev. E **76**, 041135 (2007).
[25] E. Bianchi, R. Blaak, and C. N. Likos, Patchy colloids: State of the art and perspectives, Phys. Chem. Chem. Phys. **13**, 6397 (2011).
[26] G. Wang and J. W. Swan, Surface heterogeneity affects percolation and gelation of colloids: Dynamic simulations with random patchy spheres, Soft Matter **15**, 5094 (2019).
[27] F. Sciortino and E. Zaccarelli, Equilibrium gels of limited valence colloids, Curr. Opin. Colloid Interface Sci. **30**, 90 (2017).
[28] R. Fantoni and G. Pastore, Wertheim perturbation theory: Thermodynamics and structure of patchy colloids, Mol. Phys. **113**, 2593 (2015).
[29] G. Munaò, Z. Preisler, T. Vissers, F. Smallenburg, and F. Sciortino, Cluster formation in one-patch colloids: Low coverage results, Soft Matter **9**, 2652 (2013).
[30] Q. Chen, S. C. Bae, and S. Granick, Directed self-assembly of a colloidal kagome lattice, Nature (London) **469**, 381 (2011).
[31] C.-H. Chen, R. K. Shah, A. R. Abate, and D. A. Weitz, Janus particles templated from double emulsion droplets generated using microfluidics, Langmuir **25**, 4320 (2009).
[32] Q. Chen, J. K. Whitmer, S. Jiang, S. C. Bae, E. Luijten, and S. Granick, Supracolloidal reaction kinetics of janus spheres, Science **331**, 199 (2011).
[33] A. B. Pawar and I. Kretzschmar, Fabrication, assembly, and application of patchy particles, Macromol. Rapid Commun. **31**, 150 (2010).
[34] A. Lotierzo, B. W. Longbottom, W. H. Lee, and S. A. F. Bon, Synthesis of janus and patchy particles using nanogels as stabilizers in emulsion polymerization, ACS Nano **13**, 399 (2018).
[35] G. Loget and A. Kuhn, Bulk synthesis of janus objects and asymmetric patchy particles, J. Mater. Chem. **22**, 15457 (2012).
[36] S. Ravaine and E. Duguet, Synthesis and assembly of patchy particles: Recent progress and future prospects, Curr. Opin. Colloid Interface Sci. **30**, 45 (2017).
[37] A. Gil-Villegas, A. Galindo, P. J. Whitehead, S. J. Mills, G. Jackson, and A. N. Burgess, Statistical associating fluid theory for chain molecules with attractive potentials of variable range, J. Chem. Phys. **106**, 4168 (1997).
[38] F. Sciortino, E. Bianchi, J. F. Douglas, and P. Tartaglia, Self-assembly of patchy particles into polymer chains: A parameter-free comparison between wertheim theory and Monte Carlo simulation, J. Chem. Phys. **126**, 194903 (2007).
[39] J. Zhang, B. A. Grzybowski, and S. Granick, Janus particle synthesis, assembly, and application, Langmuir **33**, 6964 (2017).
[40] E. Schöll-Paschinger, A. L. Benavides, and R. Castañeda-Priego, Vapor-liquid equilibrium and critical behavior of the square-well fluid of variable range: A theoretical study, J. Chem. Phys. **123**, 234513 (2005).
[41] E. Bianchi, J. Largo, P. Tartaglia, E. Zaccarelli, and F. Sciortino, Phase Diagram of Patchy Colloids: Towards Empty Liquids, Phys. Rev. Lett. **97**, 168301 (2006).
[42] F. Smallenburg and F. Sciortino, Liquids more stable than crystals in particles with limited valence and flexible bonds, Nat. Phys. **9**, 554 (2013).
[43] Z. Preisler, T. Vissers, F. Smallenburg, G. Munaò, and F. Sciortino, Phase diagram of one-patch colloids forming tubes and lamellae, J. Phys. Chem. B **117**, 9540 (2013).
[44] N. Kern and D. Frenkel, Fluid–fluid coexistence in colloidal systems with short-ranged strongly directional attraction, J. Chem. Phys. **118**, 9882 (2003).

[45] D. J. Earl and M. W. Deem, Parallel tempering: Theory, applications, and new perspectives, Phys. Chem. Chem. Phys. **7**, 3910 (2005).

[46] N. E. Valadez-Pérez, A. L. Benavides, E. Schöll-Paschinger, and R. Castañeda-Priego, Phase behavior of colloids and proteins in aqueous suspensions: Theory and computer simulations, J. Chem. Phys. **137**, 084905 (2012).

[47] E. M. Sevick, P. A. Monson, and J. M. Ottino, Monte Carlo calculations of cluster statistics in continuum models of composite morphology, J. Chem. Phys. **88**, 1198 (1988).

[48] A. L. R. Bug, S. A. Safran, G. S. Grest, and I. Webman, Do Interactions Raise or Lower a Percolation Threshold? Phys. Rev. Lett. **55**, 1896 (1985).

[49] S. A. Safran, I. Webman, and G. S. Grest, Percolation in interacting colloids, Phys. Rev. A **32**, 506 (1985).

[50] J. Dhont, *An Introduction to Dynamics of Colloids* (Elsevier, Amsterdam, Netherlands, 1996).

[51] F. Romano, E. Sanz, and F. Sciortino, Phase diagram of a tetrahedral patchy particle model for different interaction ranges, J. Chem. Phys. **132**, 184501 (2010).

[52] S. Marín-Aguilar, F. Smallenburg, F. Sciortino, and G. Foffi, Monodisperse patchy particle glass former, J. Chem. Phys. **154**, 174501 (2021).

[53] P. D. Godfrin, N. E. Valadez-Pérez, R. Castañeda-Priego, N. J. Wagner, and Y. Liu, Generalized phase behavior of cluster formation in colloidal dispersions with competing interactions, Soft Matter **10**, 5061 (2014).

[54] J. R. Espinosa, A. Garaizar, C. Vega, D. Frenkel, and R. Collepardo-Guevara, Breakdown of the law of rectilinear diameter and related surprises in the liquid-vapor coexistence in systems of patchy particles, J. Chem. Phys. **150**, 224510 (2019).

[55] M. G. Noro and D. Frenkel, Extended corresponding-states behavior for particles with variable range attractions, J. Chem. Phys. **113**, 2941 (2000).

[56] D. J. Jacobs, Generic rigidity in three-dimensional bond-bending networks, J. Phys. A: Math. Gen. **31**, 6653 (1998).

[57] W. Whiteley, Counting out to the flexibility of molecules, Phys. Biol. **2**, S116 (2005).

[58] G. Laman, On graphs and rigidity of plane skeletal structures, J. Eng. Math. **4**, 331 (1970).

[59] A. J. Rader, B. M. Hespenheide, L. A. Kuhn, and M. F. Thorpe, Protein unfolding: Rigidity lost, Proc. Natl. Acad. Sci. USA **99**, 3540 (2002).

[60] T. Bauer, P. Lunkenheimer, and A. Loidl, Cooperativity and the Freezing of Molecular Motion at the Glass Transition, Phys. Rev. Lett. **111**, 225702 (2013).

[61] F. Romano, C. De Michele, D. Marenduzzo, and E. Sanz, Monte Carlo and event-driven dynamics of Brownian particles with orientational degrees of freedom, J. Chem. Phys. **135**, 124106 (2011).

[62] S. Jabbari-Farouji and E. Trizac, Dynamic Monte Carlo simulations of anisotropic colloids, J. Chem. Phys. **137**, 054107 (2012).

[63] E. Sanz and D. Marenduzzo, Dynamic Monte Carlo versus Brownian dynamics: A comparison for self-diffusion and crystallization in colloidal fluids, J. Chem. Phys. **132**, 194102 (2010).

[64] F. Perrin, Mouvement Brownien d'un ellipsoide (II). Rotation libre et dépolarisation des fluorescences. Translation et diffusion de molécules ellipsoidales, J. Phys. Radium **7**, 1 (1936).